Frictional active Brownian particles

Pin Nie,[1,2] Joyjit Chattoraj,[1] Antonio Piscitelli,[1,3] Patrick Doyle,[2,4] Ran Ni,[5,*] and Massimo Pica Ciamarra[1,3,†]

[1]*School of Physical and Mathematical Science, Nanyang Technological University, Singapore 637371, Singapore*
[2]*Singapore-MIT Alliance for Research and Technology, Singapore 138602, Singapore*
[3]*CNR–SPIN, Dipartimento di Scienze Fisiche, Università di Napoli Federico II, I-80126 Naples, Italy*
[4]*Department of Chemical Engineering, Massachusetts Institute of Technology, Cambridge, Massachusetts 02139, USA*
[5]*School of Chemical and Biomedical Engineering, Nanyang Technological University, Singapore 637459, Singapore*

(Received 2 August 2020; accepted 8 September 2020; published 23 September 2020)

Frictional forces affect the rheology of hard-sphere colloids, at high shear rate. Here we demonstrate, via numerical simulations, that they also affect the dynamics of active Brownian particles and their motility-induced phase separation. Frictional forces increase the angular diffusivity of the particles, in the dilute phase, and prevent colliding particles from resolving their collision by sliding one past to the other. This leads to qualitatively changes of motility-induced phase diagram in the volume-fraction motility plane. While frictionless systems become unstable towards phase separation as the motility increases only if their volume fraction overcomes a threshold, frictional systems become unstable regardless of their volume fraction. These results suggest the possibility of controlling the motility-induced phase diagram by tuning the roughness of the particles.

DOI: 10.1103/PhysRevE.102.032612

I. INTRODUCTION

The interaction force between macroscopic objects in direct physical contact has a frictional component. In colloidal hard-sphere suspensions, direct interparticle contacts are generally suppressed by frictionless repulsive forces, of electrostatic or polymeric origin, which are needed to stabilize the suspension, as well as by lubrication forces [1]. Hence, in these systems, frictional forces are generally negligible. Recent results [2–5] have, however, shown that in colloidal systems under shear, frictional force might become relevant. This occurs as the relative velocity between contacting particles is of order $\sigma\dot{\gamma}$, with σ particle diameter and $\dot{\gamma}$ the shear rate. At large enough $\dot{\gamma}$, colliding particles become able to overcome their lubrication interaction, entering into direct physical contact. The resulting frictional forces are believed to trigger the discontinuous shear thickening [2–5] phenomenology, an abrupt increase of the shear viscosity with the shear rate.

In systems of self-propelled colloidal particles the relative velocity between colliding particles could also be high. Therefore, frictional forces could play a role in these systems by affecting their distinguishing feature, which is a motility-induced phase separation (MIPS) from a homogeneous state, to one in which a high-density liquidlike state coexists with a low-density gaslike state. While the physical origin and the features of this transition have been extensively investigated in the last few years, in both numerical model systems [6–8] as well as experimental realizations [9–12], the role of frictional forces causing colliding particles to exert torques on each other has been ignored.

In this paper, we investigate the effect of frictional forces on the motility-induced phase separation of active spherical Brownian particles (ABPs), a prototypical active matter system. In this model, hard-sphere-like particles of diameter σ are equipped with a polarity $\boldsymbol{n}$ along which they self-propel with active velocity v_a. The self-propelling directions change as $\boldsymbol{n}$ undergo rotational Brownian motion, with rotational diffusion coefficient D_r. Thermal noise also acts on the positional degree of freedom. The motility-induced phase separation of this model is controlled by two variables, the volume fraction, ϕ, and the Péclet number, $\mathrm{Pe} \equiv v_a/(D_r\sigma)$. Here we show that friction qualitatively affects the dynamical properties of ABPs, in the homogeneous phase, by enhancing the rotational diffusion while suppressing the translational one. Because of this, friction qualitative changes the spinodal line marking the limit of stability of the homogeneous phase in the ϕ-Pe plane, at high Pe. While in the absence of friction [13] the low-density spinodal line diverges at a finite volume fraction $\phi_m > 0$, in the presence of friction it diverges at $\phi_m \to 0$. In this respect, friction makes the motility-induced phase diagram of ABPs closer to that observed in most active particle systems, including dumbbells [14,15] and schematic models such as run-and-tumble particles [13], active OrnsteinUhlenbeck [16], and Monte Carlo models [17], and also closer to gas-liquid transition phase diagram in passive systems. Since the frictional interaction between colloidal scale particles can be experimentally tuned [4], our result indicates that it is possible to experimentally modulate the motility-induced phase diagram by optimising the particle roughness.

The paper is organized as follows. After describing our model in Sec. II, we compare in Sec. III the frictionless and the frictional dynamics, in the homogeneous phase, showing

*r.ni@ntu.edu.sg
†massimo@ntu.edu.sg

that friction suppresses the translational diffusivity while it enhances the rotational one. The friction dependence of the motility-induced phase diagram is discussed in Sec. IV. Section V discusses the dynamics in the phase-separated region and highlights how friction promotes the stability of active clusters and hence promotes separation.

II. NUMERICAL MODEL

We consider two- and three-dimensional suspensions of active spherical Brownian particles (ABPs) with average diameter σ (polydispersity: 2.89%) and mass m, in the overdamped limit. The equations of motion for the translational and the rotational velocities are

$$\boldsymbol{v}_i = \frac{\boldsymbol{F}_i}{\gamma} + \frac{F_a}{\gamma}\hat{\boldsymbol{n}}_i + \sqrt{2D_t^0}\boldsymbol{\eta}_i^t, \tag{1}$$

$$\boldsymbol{\omega}_i = \frac{\boldsymbol{T}_i}{\gamma_r} + \sqrt{2D_r^0}\boldsymbol{\eta}_i^r. \tag{2}$$

Here D_r^0 and $D_t^0 = D_r^0\sigma^2/3$ are the rotational and the translational diffusion coefficients, γ is the viscosity, $\gamma_r = \gamma\frac{\sigma^2}{3}$, η is Gaussian white noise variable with $\langle\eta\rangle = 0$ and $\langle\eta(t)\eta(t')\rangle = \delta(t-t')$, F_a is the magnitude of the active force acting on the particle and $\hat{\boldsymbol{n}}_i$ its direction, and $\boldsymbol{F}_i = \sum \boldsymbol{F}_{ij}$ and $\boldsymbol{T}_i = \frac{\sigma_i}{2}\sum(\hat{\boldsymbol{r}}_{ij}\times\boldsymbol{F}_{ij})$ are the forces and the torques arising from the interparticle interactions. In the absence of interaction and noise, particles move with velocity $v_a = F_a/\gamma$ and do not rotate.

We use an interparticle interaction model borrowed from the granular community, to model frictional particles. The interaction force has a normal and a tangential component, $\boldsymbol{F}_{ij} = \boldsymbol{f}_{ij}^n + \boldsymbol{f}_{ij}^t$. The normal interaction is a purely repulsive Harmonic interaction, $\boldsymbol{f}_{ij}^n = k_n(\sigma_{ij} - r_{ij})\Theta(\sigma_{ij} - r_{ij})\hat{\boldsymbol{r}}_{ij}$, $\Theta(x)$ is the Heaviside function, $\sigma_{ij} = (1/2)(\sigma_i + \sigma_j)$, $\boldsymbol{r}_{ij} = \boldsymbol{r}_i - \boldsymbol{r}_j$, and $\boldsymbol{r}_i$ is the position of particle i. The tangential force is $\boldsymbol{f}_{ij}^t = k_t\vec{\xi}_{ij}$, where $\boldsymbol{\xi}_{ij}$ is the shear displacement, defined as the integral of the relative velocity of the interacting particle at the contact point throughout the contact, and $k_t = \frac{2}{7}k_n$. In addition, the magnitude of tangential force is bounded according to Coulomb's condition: $|\boldsymbol{f}_{ij}^t| \leqslant \mu|\boldsymbol{f}_{ij}^n|$. Working in the overdamped limit, we neglect any viscous dissipation in the interparticle interaction. In the granular model, we also neglect the presence of rolling friction [18] we expect not to qualitatively affect our results, in analogy with recent findings [19] on the role of rolling friction on discontinuous shear thickening. The value of k_n is chosen to work in the hard-sphere limit, the maximum deformation of a particle being of order $\delta/\sigma \leqslant 5\times10^{-4}$. We simulate systems with $N = 10^4$, unless otherwise stated, in the overdamped limit, with integration time step $2\times10^{-8}/D_r^0$, using periodic boundary conditions. We have checked that for the considered value of N finite-size effects are negligible away from the critical point, in the range of parameters we consider. Data are collected after allowing the system to reach a steady-state via simulation lasting at least 2τ, where τ is the time at which the diffusive regime is attained we estimate from the study of the mean-square displacement.

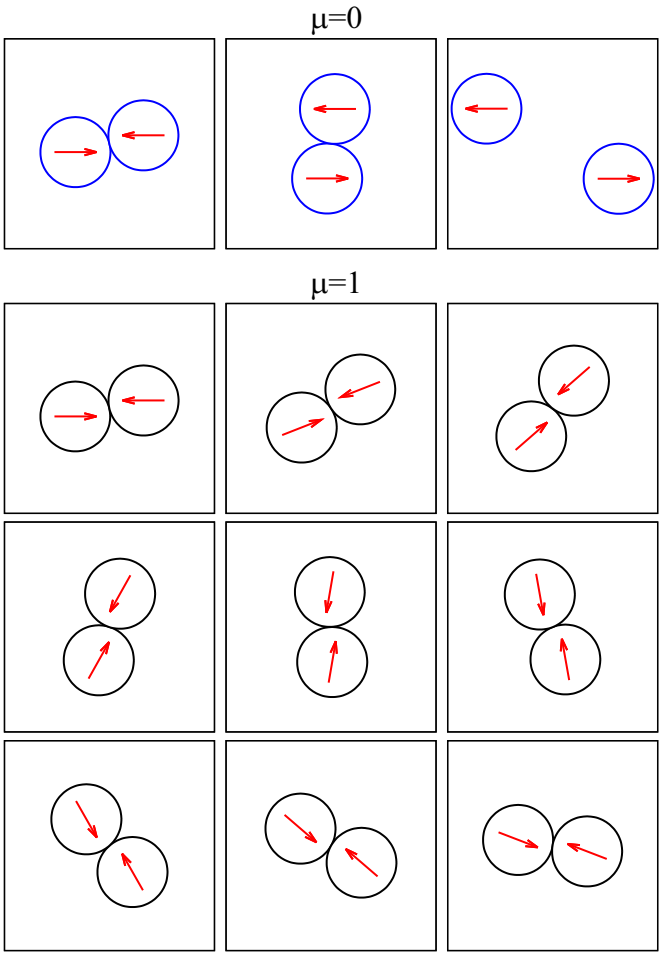

FIG. 1. Time evolution of the positions and of the self-propelling directions of two colliding particles, for frictionless (top row) and for frictional (bottom rows) particles. Time evolves from left to right and from top to bottom. In the time interval between consecutive images a free particle moves one diameter. In these simulations, we neglect both translational and rotational noise.

III. DYNAMICS IN THE HOMOGENEOUS PHASE

A. Frictional effect on the interparticle collision

To appreciate the role of friction on the properties of ABPs, we start considering how friction affects the collision between two particles. The interparticle force acting between two colliding particles generally has a component parallel to the line joining the centers of the two particles and a tangential component. In the absence of friction, this tangential component allows the particles to slide one past the other to resolve their collision, as illustrated in the upper row of Fig. 1.

In the presence of friction, particles are not free to tangentially slide one past the other. Specifically, the tangential shearing-induced an opposing frictional force that slows down the motion of the particles, and it induces their rotation. In the absence of thermal forces, or equivalently in the Pe $\to\infty$ limit, the frictional forces cause the particles to rigidly rotate around their contact point, so that they never resolve their collision, as is illustrated in the bottom rows of Fig. 1. At any finite Pe, the stochastic forces acting on the particles will

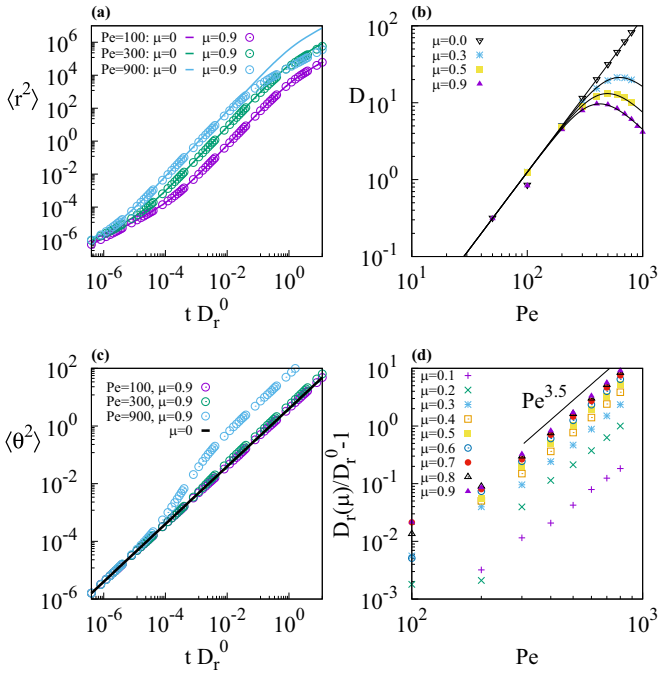

FIG. 2. Mean-square displacement (a) for the frictionless ($\mu = 0$, full lines) and the frictional dynamics ($\mu = 0.9$, symbols) for selected values of the Péclet number. At large Pe friction reduces the time at which the dynamics enter the asymptotic diffusive regime and hence suppresses the diffusion coefficient (b). The mean-square angular displacement (c) is enhanced by the frictional force, at times larger than the interparticle collision time. This leads to an increase of the rotational diffusivity (d) scaling as $\mu^2 \mathrm{Pe}^x$, with $x \simeq 3.5$. Lines in panel (b) are one-parameter fits to the theoretical prediction of Eq. (4) where $x = 3.5$ is held constant. In all panels, $\phi = 0.1$.

be able to break their contact and hence the frictional forces, allowing the particles to resolve their collision. We do expect, therefore, that friction may affect the physics of ABP at high Pe, inducing a non-negligible rotation of the self-propelling directions of colliding particles.

B. Dilute phase

We start describing the effect of friction on the MIPS, comparing the dynamics of frictionless and frictional systems in the homogeneous phase. Figure 2(a) illustrates the frictionless and the frictional mean-square displacement, at different Péclet numbers, for volume fractions in the gas phase. In the absence of friction (full lines) the mean-square displacement exhibits a crossovers from a diffusive to a superdiffusive regime at $t \simeq 6D_t^0/v_a^2$, and from the superdiffusive to the asymptotic diffusive regime at $t = 1/D_r^0$ [6]. In the presence of friction (symbols), similar behavior is observed, but the system enters the diffusive regime on a smaller timescale. Consequently, the translational diffusivity is also reduced as illustrated in Fig. 2(b). This finding is rationalized investigating the mean-square angular displacement [Fig. 2(c)] and the dependence of the rotational diffusivity D_r on Pe [Fig. 2(d)]. Indeed, these quantities clarify that friction enhances the rotational diffusion of the particles, hence reducing the timescale at which the system enters the asymptotic translational diffusive regime.

We rationalize how friction leads to an increase of the rotational diffusivity, considering that in a collision a frictional particle experiences a torque, which induces the rotation of its self-propelling direction. More quantitatively, in the overdamped limit, the rotation $\Delta\theta_i$ induced by a collision is proportional to the induced torque and the duration of the contact. If the contacts are at their critical Coulomb value, the typical torque magnitude is $\sigma f^t \propto \mu f^n \propto \mu \mathrm{Pe}$, and the mean-squared angular displacement induced by a collision of duration t_{coll} is $\langle \Delta\theta_i^2 \rangle \propto \mu^2 \mathrm{Pe}^2 t_{\mathrm{coll}}^2$. At low density consecutive torques experienced by a particle are uncorrelated, and the number of collisions per unit time is proportional to Pe. Hence, assuming $t_{\mathrm{coll}} \propto \mathrm{Pe}^q$, we predict for the rotational diffusivity

$$D_r(\mathrm{Pe}, \mu) = D_r^0 + \alpha \mu^2 \mathrm{Pe}^x \tag{3}$$

with $x = 3 + 2q$. Our numerical results of Fig. 2(d) indicate $x \simeq 3.5$. These results indicate that the average duration of an interparticle collision slightly grows with the Péclet number, $t_{\mathrm{coll}} \propto \mathrm{Pe}^{1/4}$. We qualitatively rationalize the dependence of the collision duration on the Péclet number considering that Pe controls the ratio between the frictional forces, which protract the duration of contacts, and the thermal ones, which eventually allow particles to resolve their collision. We have indeed observed in Fig. 1 that in the $\mathrm{Pe} \to \infty$ limit collisions are not resolved, so that $t_{\mathrm{coll}} = \infty$.

The dependence of the rotational diffusion coefficient on Pe and on μ allows us also to rationalize the nonmonotonic behavior of the diffusivity observed in Fig. 2(b). Indeed, in the $\phi \to 0$ limit the long-time mean-square displacement of an active particle is $\Delta r^2(t) = 6D_t^0 t + \frac{v_a^2}{D_r} t$. At a small but finite density ϕ, we therefore expect

$$D(\mathrm{Pe}, \mu) = c(\phi)\left[D_t^0 + \frac{\sigma^2}{6}\frac{(D_r^0)^2}{D_r(\mathrm{Pe}, \mu)}\mathrm{Pe}^2\right] \tag{4}$$

with $c(\phi)$ a constant of order one, $D_r(\mathrm{Pe}, \mu)$ is given by Eq. (3). Equation (4) well describes the data of Fig. 2(b), with $c(\phi = 0.1) \simeq 0.8$. Hence, the diffusivity grows as Pe^2 at small Pe, and decreases as Pe^{2-x} at large Pe.

IV. FRICTIONAL MIPS

We have investigated the motility phase diagram as a function of the friction coefficient μ, of the volume fraction ϕ, and of the Péclet number $\mathrm{Pe} \equiv v_a \tau_B/\sigma$, where v_a is the particle velocity in the $\phi \to 0$ limit, σ is the average particle diameter, and $\tau_B = 1/D_r^0$ is the Brownian time, D_r^0 being the rotational diffusion coefficient of the self-propelling directions in the absence of friction. We have determined the phase diagram considering the systems to be phase separated when the distribution of the local density exhibits two peaks, at the end of relative short simulations. Indeed, this ensures that phase separation has occurred via spinodal decomposition, rather than via nucleation, as we previously verified [20]. We discuss here results obtained in three spatial dimensions.

In the absence of friction, our results are in qualitative agreement with previous investigations. The increase of the Péclet number drives the phase separation of the system, but

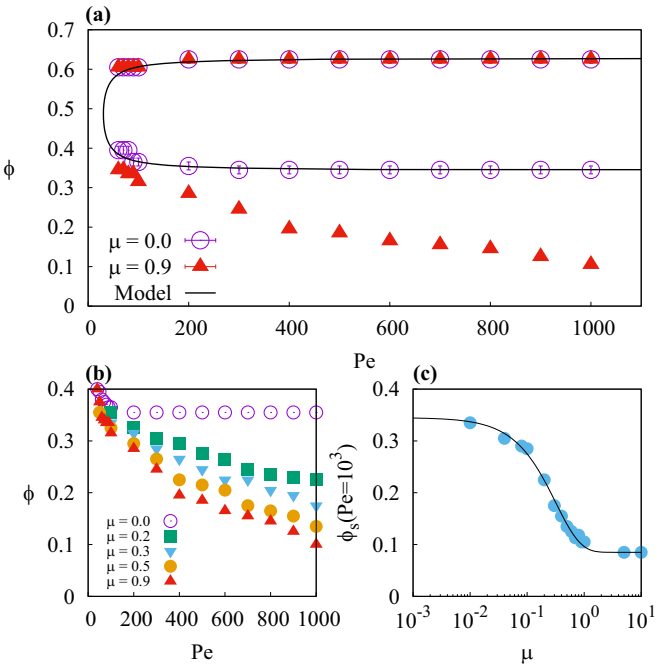

FIG. 3. The phase diagrams of frictionless (circles) and of frictional (triangles) ABPs are compared in (a). The full line, a parabola, is the theoretical prediction of Ref. [20], for frictionless systems. At high Pe the low-density critical line saturates to a constant value in the absence of friction, while it vanishes in the frictional case. This occurs for all values of the friction coefficient, as shown in panel (b). At a given Pe, the critical volume fraction at which phase separation occurs varies with friction as $\phi_s(\mu) = \phi_s(\infty) + \Delta\phi_s e^{-\mu/\mu_c}$. For $\mathrm{Pe} = 10^3$ (c) we find $\phi_s(\infty) = 0.085(3)$, $\Delta\phi_s = 0.26(2)$, and $\mu_c = 0.32(1)$.

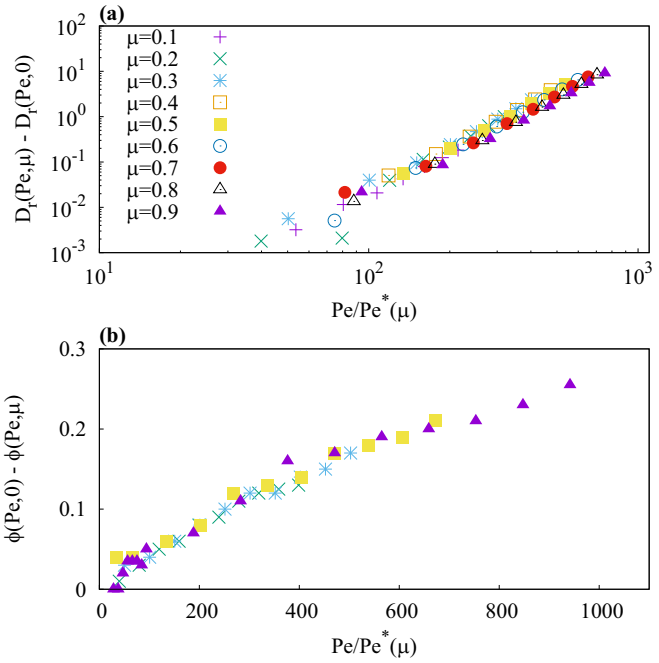

FIG. 4. Friction leads to an increase of the rotational diffusivity scaling as $D_r(\mathrm{Pe}, \mu) - D_r(Pe, 0) \propto \mathrm{Pe}^* \propto \mu^{-4/7}$ (a). The difference between the frictionless and the frictional low-density critical lines [see Fig. 3(b)] is also controlled by Pe^* (b).

only for volume fractions above a critical value [7,21–23], as illustrated in Fig. 3(a) (circles).

We highlight how friction influences this scenario by also illustrating in Fig. 3(a) the spinodal line for $\mu = 0.9$ (triangles). The figure reveals that friction does not appreciably influence the high-density spinodal line, while it strongly affects the low-density line does. In particular, while $\phi_s(\mathrm{Pe}, \mu = 0)$ reaches a plateau as Pe increases, $\phi_s(\mathrm{Pe}, 0)$ monotonically decreases with Pe. A similar effect of friction has been reported on the volume fraction of static granular packing [24,25]. Hence, the effect of friction becomes more relevant on increasing Pe, as we anticipated in Sec. III A.

Figure 3(b) further investigates this dependence illustrating the low-density spinodal line for different values of the friction coefficient. Regardless of the μ value, the spinodal line decreases on increasing Pe or μ. Figure 3(c) illustrates the value of the lower-spinodal line, at $\mathrm{Pe} = 10^3$, as a function of μ. The figure reveals that this value exponentially decreases with μ, approaching a limiting value. This exponential dependence is rationalized considering that the frictional forces, whose magnitude scale as $\mu v_a \propto \mu\mathrm{Pe}$, can be disrupted by thermal forces that have a constant magnitude through an activated process. Since the associated Boltzmann factor $\exp(-\mu\mathrm{Pe})$ vanishes in the $\mathrm{Pe} \to \infty$ limit, so thus the spinodal line, for $\mu > 0$. Hence, the frictionless case appears as a singular one.

To quantitatively rationalize the interplay between friction and Péclet number, we consider that according to Eq. (3) frictional forces play a role for $\mathrm{Pe} > \mathrm{Pe}^* \propto \mu^{-4/7}$, as found imposing $\mu(\mathrm{Pe}^*)^x \propto D_r^0$. Indeed, we show in Fig. 4(a) that, when plotted versus $\mathrm{Pe}/\mathrm{Pe}^*$, rotational diffusivity data corresponding to different values of the friction coefficient nicely collapse. Accordingly, the frictional critical line $\phi_c(\mathrm{Pe}, \mu)$ coincides with the frictionless one for $\mathrm{Pe} < \mathrm{Pe}^*(\mu)$, while conversely it deviates from it. We confirm this expectation in Fig. 4(b), which illustrates that the distance between the frictionless and the frictional critical lines, $\phi(\mathrm{Pe}, 0) - \phi_c(\mathrm{Pe}, \mu)$, scales as $\mathrm{Pe}/\mathrm{Pe}^*(\mu)$.

V. DYNAMICS IN THE PHASE SEPARATED PHASE

Friction significantly stabilizes phase-separated configurations, thus expanding the coexistence region in the ϕ-Pe plane. To understand how friction stabilized an active cluster, we start by considering a frictional simulation for parameter values at which phase separation occurs, $\mathrm{Pe} = 500$, $\phi = 0.2$, and $\mu = 0.9$. Also, for ease of visualization, we consider a small two-dimensional system, with $N = 500$ particles, so that in the steady state we readily observe the formation of a single cluster. This is illustrated in Fig. 5(a). In this and the other panels of Fig. 5, we also illustrate the active velocity field evaluated on a square grid with lattice spacing $\sim 1.5\sigma$. We associate to each grid point the average active velocity of the particles in a circle of radius $\simeq 2.2\sigma$. In the figure, we show the values of the field on the grid points that average over at least five particles. We use the configuration Fig. 5(a) as the initial configuration of two different simulations, a frictionless ($\mu = 0$) and a frictional one ($\mu = 0.9$).

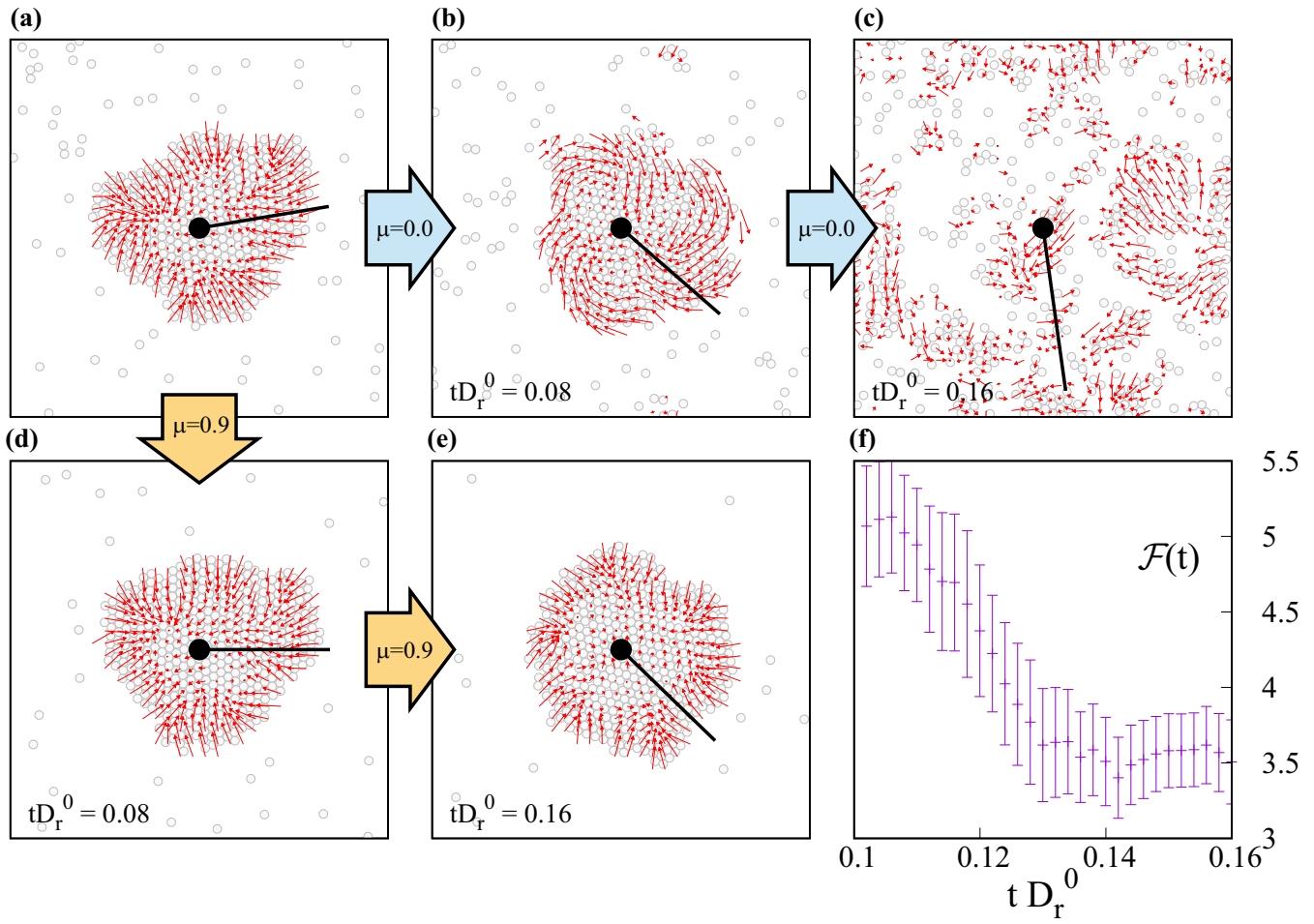

FIG. 5. Evolution of a two-dimensional cluster of ABPs in the absence (a–c) and in the presence (a, d, e) of frictional forces. The red arrows show the active force field (see Methods). In all plots, the central black circle identifies the position of the particle closer to the center of mass of the cluster, in the initial configuration. We emphasize the rotational motion of the cluster, drawing a line connecting the central particle and another particle of the cluster. Both with and without friction the cluster rigidly rotates around its center of mass. In the absence of friction, the rotation of the cluster makes the active velocities parallel to the cluster surface (b) inducing a cluster instability (c). We see in panel (f) that, in the absence of friction, as the cluster rotates, the average interaction force that contrasts the motion along the direction of the self-propelling forces decreases, fluctuating around a value characteristic of the homogeneous phase once the cluster breaks. In the presence of friction, the cluster rotation induces that of the self-propelling directions, and the cluster remains stable (d, e). For these illustrative two-dimensional simulations $N = 500$, $\mathrm{Pe} = 500$, $\phi = 0.2$, and $\mu = 0.0, 0.9$.

Figures 5(a)–5(c) show that in the absence of friction the cluster becomes unstable and disintegrates upon rotation. The instability occurs as the rotation makes the self-propelling velocities tangential to the cluster surface. We have verified that the system becomes macroscopically unstable by investigating the magnitude of the forces which oppose the motion of the particles in their self-propelling directions $\mathcal{F}(t) = -\frac{1}{NF_a}\frac{d}{d\alpha}U(\boldsymbol{r}(t) + \alpha\hat{\boldsymbol{n}})|_0$, where U is the elastic energy of the system and $\hat{\boldsymbol{n}}$ is the director of the active velocity field, normalized by the magnitude F_a of the active force acting on each particle and by the number of particles N. Figure 5(f) shows that $\mathcal{F}(t)$ quickly decreases as the cluster rotates, reflecting the development of the instability.

Friction promotes phase separation by suppressing this rotational-induced instability of active clusters. This is illustrated in Figs. 5(a), 5(d), and 5(e). The frictional cluster is stable because its rotation induces that of the self-propelling directions of its particles. Indeed, we observe in Figs. 5(a), 5(d), and 5(e) the active velocities always point towards the center of the cluster. This tendency is more pronounced the higher the frictional forces, and hence at large μ and large Pe. As a consequence of this process, while in the absence of friction active clusters quickly disintegrate as they start rotating, in frictional ABPs one observes long-lasting active clusters that perform many revolutions before eventually breaking apart. In this respect, frictional ABPs behave as active dumbbells [14,15].

From the decay of $\mathcal{F}(t)$ it is possible to extract the lifetime of the considered cluster. For the cluster illustrated in Fig. 5, This lifetime is $\simeq 0.12 D_r^0$ in the absence of friction, as apparent from Fig. 5(f). For this cluster, we have observed the lifetime quickly grow as the friction coefficient increases, reaching values beyond our simulation capabilities for $\mu \simeq 0.2$. This result strongly suggests that frictional clusters break as thermal fluctuations succeed in inducing the relative rotation of the contacting cluster.

VI. DISCUSSION

We have investigated the stability phase diagram of frictionless active Brownian particles and rationalized its spinodal line within a kinetic model. In this model, the finite value of the lower-spinodal line in the Pe limit, in the absence of friction, results from the competition of two processes. Phase separation is promoted by the collisions of the particles in the homogeneous phase, which may trigger the agglomeration. Being related to the particle velocity, this process leads to a flux of particles $j_g \propto \mathrm{Pe}$ from the dilute to the dense phase. The dilute phase is promoted by the process that allows particles to resolve their collisions. At low Pe, particles mainly resolve their collision by rotating their self-propelling direction. In the high-Pe limit we are interested in, conversely, particles resolve their collisions by sliding past one to the other, as illustrated in Fig. 1, before their self-propelling direction changes. This sliding-detaching mechanisms, also driven by the motility, leads to a flux of particles from the dense to the less-dense phase, $j_{\mathrm{sd}} \propto \mathrm{Pe}$. Since both j_g and j_{sd} are proportional to the Péclet number, the spinodal line results tend not to depend on it.

Within this context, the role of friction is rationalized considering its influence on these contrasting fluxes. In Sec. III B we demonstrated that friction influences the homogeneous phase by increasing the rotational diffusivity. This increase does not affect the typical velocity of the particles and hence the flux j_g. On the other hand, we have found friction to have suppressed the ability of two particles to slide one past the other, to resolve their collision, in Sec. III A. Similarly, in the phase-separated phase, friction stabilizes an active cluster, which would conversely disintegrate upon rotation, as discussed in Sec. V. The balance between j_g and j_{sd}, therefore, leads to a friction-dependent spinodal line with the coexistence region widening on increasing the friction coefficient.

That the suppression of the sliding detaching mechanism leads to a widening of the coexistence region is consistent with previous findings. In the context of frictionless spherical particles, the sliding detaching mechanisms are suppressed when the dynamics is investigated via Monte Carlo simulations, which are unable to account for the cooperative displacement of colliding particles. Consistently, in these simulations the spinodal line is found to vanish in the $\mathrm{Pe} \to \infty$ limit [16,17]. The sliding detaching mechanisms are also suppressed in the system of active anisotropic particles. Indeed, these particles cannot rotate independently when in a dense cluster, which implies that an active cluster of anisotropic particles does not destabilize when rotating, as in frictional spherical particles (see Fig. 5). Consistently, the spinodal line of frictionless dumbbells does also vanish [14,15] in the $\mathrm{Pe} \to \infty$ limit.

Interestingly, we notice that long-lived rotating clusters have also been observed in experiments of active thermophoretic particles [9–11]. These clusters might perform several revolutions before restructuring. While it is understood that these clusters might be stabilized by the attractive phoretic attraction between the particles [10,11,26], it has been suggested that this attraction is not always present [9]. In these circumstances, friction might be a concurring stabilizing factor, as one could experimentally ascertain investigating whether the self-propelling directions of the particles rotate with the cluster itself.

Regardless, frictional forces could be enhanced by acting on the roughness of the particles [4], suggesting that friction could be used as a control parameter to experimentally tune the motility-induced phase diagram.

ACKNOWLEDGMENTS

We acknowledge support from the Singapore Ministry of Education through the Academic Research Fund MOE2017-T2-1-066 (S) and are grateful to the National Supercomputing Centre (NSCC) for providing computational resources.

[1] J. N. Israelachvili, *Intermolecular and Surface Forces*, 3rd ed. (Academic Press, Burlington, MA, 2011), p. 704.

[2] B. M. Guy, M. Hermes, and W. C. K. Poon, Towards a Unified Description of the Rheology of Hard-Particle Suspensions, Phys. Rev. Lett. **115**, 088304 (2015).

[3] C. Clavaud, A. Bérut, B. Metzger, and Y. Forterre, Revealing the frictional transition in shear-thickening suspensions., Proc. Nat. Acad. Sci. USA **114**, 5147 (2017).

[4] C.-P. Hsu, S. N. Ramakrishna, M. Zanini, N. D. Spencer, and L. Isa, Roughness-dependent tribology effects on discontinuous shear thickening., Proc. Nat. Acad. Sci. USA **115**, 5117 (2018).

[5] T. Kawasaki and L. Berthier, Discontinuous shear thickening in Brownian suspensions, Phys. Rev. E **98**, 012609 (2018).

[6] G. S. Redner, M. F. Hagan, and A. Baskaran, Structure and Dynamics of a Phase-Separating Active Colloidal Fluid, Phys. Rev. Lett. **110**, 055701 (2013).

[7] A. Wysocki, R. G. Winkler, and G. Gompper, Cooperative motion of active Brownian spheres in three-dimensional dense suspensions, Europhys. Lett. **105**, 48004 (2014).

[8] Y. Fily and M. C. Marchetti, Athermal Phase Separation of Self-Propelled Particles with No Alignment, Phys. Rev. Lett. **108**, 235702 (2012).

[9] I. Buttinoni, J. Bialké, F. Kümmel, H. Löwen, C. Bechinger, and T. Speck, Dynamical Clustering and Phase Separation in Suspensions of Self-Propelled Colloidal Particles, Phys. Rev. Lett. **110**, 238301 (2013).

[10] J. Palacci, S. Sacanna, A. P. Steinberg, D. J. Pine, and P. M. Chaikin, Living crystals of light-activated colloidal surfers, Science **339**, 936 (2013).

[11] I. Theurkauff, C. Cottin-Bizonne, J. Palacci, C. Ybert, and L. Bocquet, Dynamic Clustering in Active Colloidal Suspensions with Chemical Signaling, Phys. Rev. Lett. **108**, 268303 (2012).

[12] F. Ginot, I. Theurkauff, F. Detcheverry, C. Ybert, and C. Cottin-Bizonne, Aggregation-fragmentation and individual dynamics of active clusters, Nat. Commun. **9**, 696 (2018).

[13] M. E. Cates and J. Tailleur, Motility-induced phase separation, Annu. Rev. Condens. Matter Phys. **6**, 219 (2015).

[14] A. Suma, G. Gonnella, D. Marenduzzo, and E. Orlandini, Motility-induced phase separation in an active dumbbell fluid, Europhys. Lett. **108**, 56004 (2014).

[15] I. Petrelli, P. Digregorio, L. F. Cugliandolo, G. Gonnella, and A. Suma, Active dumbbells: Dynamics and morphology in the coexisting region, Eur. Phys. J. E **41**, 128 (2018).

[16] J. U. Klamser, S. C. Kapfer, and W. Krauth, Thermodynamic phases in two-dimensional active matter, Nat. Commun. **9**, 5045 (2018).

[17] D. Levis and L. Berthier, Clustering and heterogeneous dynamics in a kinetic Monte Carlo model of self-propelled hard disks, Phys. Rev. E **89**, 062301 (2014).

[18] Z. Shojaaee, L. Brendel, J. Török, and D. E. Wolf, Shear flow of dense granular materials near smooth walls. II. Block formation and suppression of slip by rolling friction, Phys. Rev. E **86**, 011302 (2012).

[19] A. Singh, C. Ness, R. Seto, J. J. de Pablo, and H. M. Jaeger, Shear Thickening and Jamming of Dense Suspensions: The "Roll" of Friction, Phys. Rev. Lett. **124**, 248005 (2020).

[20] P. Nie, J. Chattoraj, A. Piscitelli, P. Doyle, R. Ni, and M. P. Ciamarra, Stability phase diagram of active Brownian particles, Phys. Rev. Res. **2**, 23010 (2020).

[21] J. Stenhammar, D. Marenduzzo, R. J. Allen, and M. E. Cates, Phase behavior of active Brownian particles: The role of dimensionality, Soft Matter **10**, 1489 (2014).

[22] D. Levis, J. Codina, and I. Pagonabarraga, Active Brownian equation of state: Betastability and phase coexistence, Soft Matter **13**, 8113 (2017).

[23] P. Digregorio, D. Levis, A. Suma, L. F. Cugliandolo, G. Gonnella, and I. Pagonabarraga, Full Phase Diagram of Active Brownian Disks: From Melting to Motility-Induced Phase Separation, Phys. Rev. Lett. **121**, 098003 (2018).

[24] L. E. Silbert, Jamming of frictional spheres and random loose packing, Soft Matter **6**, 2918 (2010).

[25] M. P. Ciamarra, R. Pastore, M. Nicodemi, and A. Coniglio, Jamming phase diagram for frictional particles, Phys. Rev. E **84**, 041308 (2011).

[26] B. Liebchen and H. Löwen, Which interactions dominate in active colloids? J. Chem. Phys. **150**, 61102 (2019).